A bio-based hyperbranched flame retardant for epoxy resins

Junheng Zhang[a,*], Xiaoqian Mi[a], Shiyuan Chen[a], Zejun Xu[a], Daohong Zhang[a,*], Menghe Miao[b], Junsheng Wang[c]

[a] Key Laboratory of Catalysis and Energy Materials Chemistry of Ministry of Education & Hubei Key Laboratory of Catalysis and Materials Science, South-Central University for Nationalities, Wuhan 430074, China
[b] CSIRO Manufacturing, 75 Pigdons Road, Waurn Ponds, Victoria 3216, Australia
[c] Tianjin Fire Research Institute of the Ministry of Emergency Management, Tianjin 300381, China

HIGHLIGHTS

- A novel bio-based hyperbranched flame retardant was prepared from itaconic anhydride.
- It significantly improved both toughness and flame retardancy of epoxy resins at low phosphorus content.
- It exhibited both gas and condensed phase flame retardant mechanisms.
- Epoxy thermosets with hyperbranched flame retardant scored V-0 rating in the UL-94 test.
- Limiting oxygen index of epoxy resin increased to 36.3%.

GRAPHICAL ABSTRACT
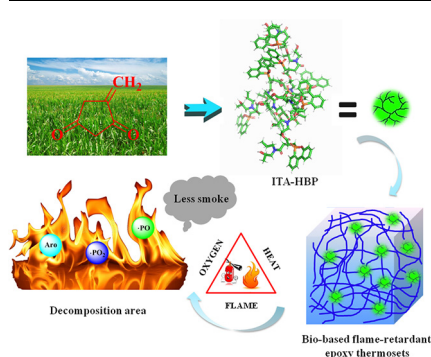
ARTICLE INFO

ABSTRACT

A novel hyperbranched flame-retardant polymer (referred to as ITA-HBP) was synthesized from itaconic anhydride as a renewable starting material. Upon the incorporation of ITA-HBP, both the toughness and flame-retarding ability of epoxy resins with low phosphorus contents increased simultaneously increased the toughness and flame retardant properties of epoxy resin with low phosphorus contents. The impact strength, fracture toughness and fracture energy of the epoxy resins are significantly enhanced by 133.2%, 78.7% and 124.7% respectively due to the *in situ* reinforcing and toughening effects induced by ITA-HBP. At the same time, the incorporated ITA-HBP exhibited a remarkable flame-retarding activity in the gas phase due to the production of phosphorus radicals and in the condensed phase due to the formation of a phosphorus-rich char layer of the epoxy resin. The addition of ITA-HBP considerably reduced the peak heat release rate, total heat release and smoke release of the epoxy resin. At a phosphorus content of 0.26 wt%, the ITA-HBP/epoxy thermosets scored V-0 rating in the UL-94 test and showed a limiting oxygen index of 36.3%.

1. Introduction

Epoxy resins are the most widely used thermosets, which are extensively applied in adhesives, insulation materials, coatings as well as structural composites to take advantage of their excellent chemical resistance, mechanical performance, adhesion properties, their comparatively low cure shrinkage and high electrical insulation properties [1–3]. However, epoxy resins poorly resist crack initiation and

propagation because of their highly cross-linked structure, which limits their application in some high-performance engineering materials [4,5]. Over the past few decades, several strategies, including the incorporation of rubbers, thermoplastics and nanofillers [6–8], have been used to toughen epoxy resins. The added rubbers or thermoplastics can significantly improve the toughness of epoxy resin. However, the improvement in toughness is usually accompanied bythe reduction of thermal stability and modulus. The incorporated nanofillers inevitably increase the viscosity of the epoxy matrix and dispersion of nanofillers, which is a major problem need to be overcome. Hyperbranched polymers have been shown to have great potential as modifiers of epoxy resins [9–11]. Santiago, et al., studied the effect of hyperbranched poly (ethyleneimine) on the thermomechanical and shape-memory properties of epoxy esins; they showed that hyperbranched poly (ethyleneimine) significantly improves the impact strength of epoxy thermosets [12]. Wang et al. synthesized a series of hyperbranched epoxy resins with a controlled epoxy equivalent weight through thiol-ene click reaction, which could effectively toughen and reinforce DGEBA [13].

Similar to other synthetic organic polymeric materials, epoxy resins are highly flammable, which limits their application in architectural and electronic materials [14–16]. Various methods have been proposed to improve the flame retardancy of epoxy resins, including the incorporation of boron, phosphorus, nitrogen and silicon containing compounds and composites [17–21]. Among various additives, 9,10-dihydro-9-oxa-10-phosphaphenanthrene-10-oxide (DOPO) and its derivatives have been widely utilized as efficient flame retardants in epoxy resins [22–24]. The P-H bond of hydrogen phosphonates or phosphinates can react with the epoxide group and the so-formed covalent bonds between the additive and the epoxy polymer chains render the epoxy resins fire resistant. Shi, et al., designed a phosphorus-containing halogen-free ionic liquid ([Dmim]Tos) as a flame retardant for epoxy resins. The added [Dmim]Tos not only improved the flame-retarding property of the epoxy resins but also their mechanical properties, while their transparency was maintained [25]. Zhang, et al., synthesized a P-P synergy flame retardant (DOPO-PEPA) and incorporated into an epoxy resin. The resulting blends scored UL94 V-0 rating and their limiting oxygen index (LOI) was found to be 35% [26]. Recently, several researchers have developed highly efficient flame retardants with low phosphorus contents. Jian, et al., reported a P/N/S containing analogue (DOPO-ABZ). The resulting epoxy/DOPO-ABZ thermosets with 0.64 wt% phosphorus content scored UL-94 rating, with their LOI being 33.5% [27]. Wang, et al., constructed a flame-retardant epoxy resin with a highly efficient flame retardant compound (DOPO-THPO). The flame retardant epoxy resin containing DOPO-THPO with low phosphorus loading (0.33 wt%) scored V-0 rating with its LOI being 30% [28]. Hyperbranched flame retardant is a new type of flame retardants; which is considered as a highly effective flame retardant [29]. Ma, et al., reported a hyperbranched poly (aminomethylphosphine oxide-amine) (HPAPOA) modifier for epoxy resins with simultaneously enhanced toughness and fire safety [30]. The epoxy resins paseed V-0 rating and acquired LOI value of 30.7 with 3.0 wt% HPAPOA. However, some of these compounds, are synthesised from petroleum-based materials. Therefore there is a huge interest in developing a bio-renewable or environmentally friendly flame retardants.

With growing environmental concerns, much of the research efforts have now shifted to the use of bio-based materials for the preparation of flame-retardant epoxy resins. A number of bio-renewable materials, such as itaconic acid, cyclodextrins, vanillin and phloroglucinol [31–34], have been used as flame retardants in epoxy resins. Zhao, et al., incorporated a bio-based flame retardant derived from β-cyclodextrin and phenylphosphonicdiamide into the epoxy resin and demonstrated improved flame retardancy and thermal stability of the epoxy resin [35]. Wang, et al., prepared a flame retardant epoxy resin based on a lignin derivative vanillin, which showed excellent flame retardancy with a LOI value of 32.8% and scored UL-94V0 rating [36].

Further, itaconic anhydride (ITA) can be produced from renewable resources [37,38]. Okuda, et al., synthesized poly (lactic acid) copolymers with itaconic anhydride and lactic acid, with molecular weights ranging up to 1.61×10^5 [39]. Joshua, et al., reported copolymers based on itaconic anhydride and methacrylate-terminated poly(L-lactic acid) with itaconic anhydride content ranging from 85 to 15 mol % [40]. Yamaguchi, et al., designed bio-based polyesters from itaconic anhydride, which can be used as macromonomers, telechelics and crosslinking reagents [41].

Here we present a novel bio-based hyperbranched polymer (ITA-HBP) by employing ITA and DOPO, which simultaneously improved the toughness and flammability of the epoxy resin at low phosphorus contents. Flame-retardant retardant epoxy thermosets were subsequently prepared by introducing ITA-HBP into the epoxy resin. The thermal properties, mechanical performance, morphology and flame retardant mechanism of the modified epoxy resins were investigated. The introduction of ITA-HBP substantially improved the flame retardancy of the epoxy resin, with the modified resin showing significant decreases in the total heat release and smoke production. Combustion of the flame-retardant epoxy resin resulted in a more compact and expanded residual char than that obtained from the parent epoxy resin.

2. Experimental

2.1. Materials

Reagent grade Reagent grade ITA (95%), DOPO (97%), diisopropanolamine (DIPA, 98%), 4,4′-diaminodiphenylmethane (DDM, 98%) and *p*-toluenesulfonic acid (TsOH, 98%) were supplied by Aladdin Industrial Corporation and were used without further purification. The diglycidyl ether of bisphenol-A (DGEBA) epoxy resin (epoxide equivalent weight of 196 g/eq) was obtained from the Baling Petrochemical Company, Inc. China.

2.2. Synthesis of DOPO-ITA

ITA (0.1 mol) and DOPO (0.1 mol) were dissolved in tetrahydrofuran (THF, 100 mL) under stirring at 50 °C and refluxed for 6 h. Then, the reaction mixture was steamed using a rotary evaporator. The obtained powder (DOPO-ITA) was washed with ethanol and dried overnight at 50 °C in a vacuum oven (yield, 94.2%).

2.3. Synthesis of bio-based hyperbranched polymers (ITA-HBP)

First, 29.54 g of DOPO-ITA (0.09 mol), 13.19 g of DIPA (0.1 mol), 0.43 g of *p*-toluenesulfonic acid, and 50 mL of N,N-dimethylformamide were mixed in a 250 mL three-necked round-bottom flask equipped with a reflux condenser. The reactants were heated at 120 °C for 6 h under overhead mechanical stirring. The resultant product ITA-HBP (yield, 93.6%) was obtained after decompressing distillation and drying at 80 °C overnight in a vacuum oven. The synthesis route of ITA-HBP is illustrated in Scheme 1.

2.4. Preparation of flame-retardant epoxy thermosets

Epoxy thermosets prepared with various contents of ITA-HBP are listed in Table 1. The epoxy thermosets were cured with DDM at a 100: 26 wt ratio. First, ITA-HBP and DDM were added to DGEBA and dispersed evenly at 80 °C through mechanical stirring to obtain a transparent and uniform mixture. The mixture was then transferred to silicone rubber moulds and cured at 80 °C for 2 h and 150 °C for 2 h. After that, all the samples were cooled to room temperature and removed from the moulds.
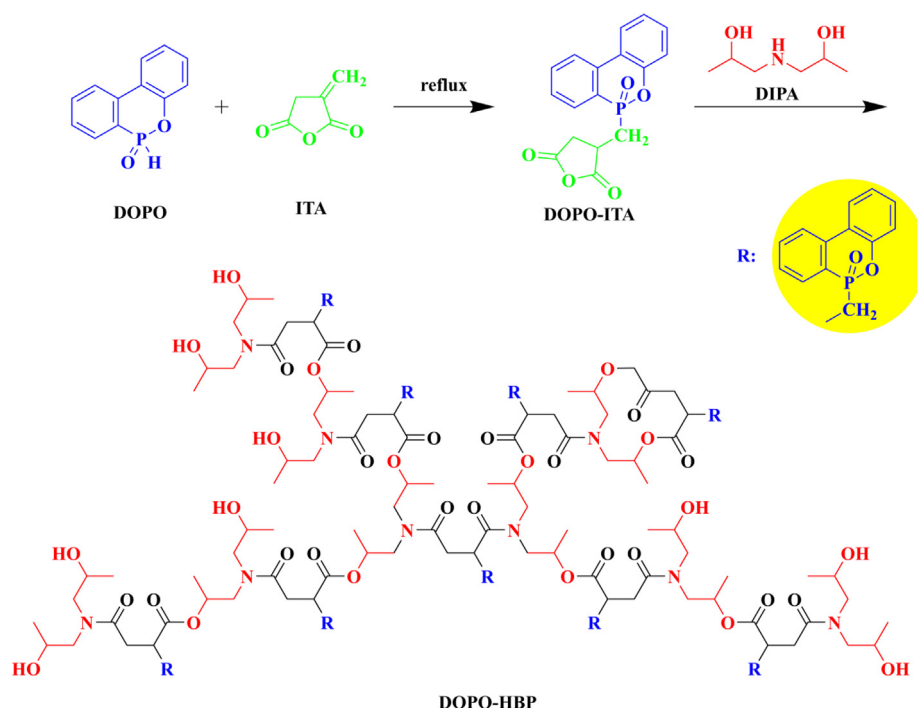
Scheme 1. Synthetic route of ITA-HBP.

Table 1
Formulations of epoxy thermosets.

Samples	Composition (phr)			Content of ITA-HBP (wt%)	Content of P (wt%)
	DGEBA	DDM	ITA-HBP		
EP0	100	26	0	0	0
EP5	100	26	5	3.82	0.26
EP10	100	26	10	7.35	0.48
EP15	100	26	15	10.64	0.72
EP20	100	26	20	13.70	0.93

2.5. Characterization

^{1}H NMR spectra were acquired using a Bruker Avance III-400 NMR spectrometer in DMSO-d_6. ^{31}P NMR spectra were measured on a JEOL JNM-ECZ600R spectrometer (600 MHz). Fourier- transform infrared (FTIR) spectra were collected on a Bruker Vertex 70 FT-IR spectrometer in the range of 400–4000 cm^{-1}. The molecular weight was recorded on a gel permeation chromatography system consisting of a Waters 1525 pump. DMF was used as the eluent. Thermogravimetric analysis (TGA) was performed on a NETZSCH 209F3 thermogravimetric analyzer (NETZSCH Gerätebau GmbH.) under air atmosphere. The samples were heated from room temperature to 700 °C at a heating rate of 10 °C/min. Dynamic mechanical analysis (DMA) was carried out using a DMA Q800 (TA Instrument, USA) at the frequency of 1 Hz and amplitude of 20 μm. The samples were heated from 35 to 300 °C in the single cantilever mode at a heating rate of 10 °C/min. The samples used for these measurements were 60.0 mm-long, 4.0 mm-thick, and 8.0 mm-wide. Tensile properties were evaluated using a universal tester (GOTECH AI-700 M, GOTECH testing Machines Inc., China) according to ASTM D638 at a crosshead speed of 2 mm/min. Flexural tests were conducted using GOTECH AI-700 M (GOTECH testing Machines Inc., China) according to ASTM D790. The impact properties were evaluated using a GT-7045-MDL impact tester (GOTECH, China) with a 2.75 J pendulum. The single-edge notched bend test was performed using a universal tensile machine (AI-700 M, Gotech Testing Machines Inc., China), according to ASTM D5045 at a loading rate of 1 mm/min. A sharp crack was introduced at the notch tip by tapping it with a fresh razor blade. The fracture toughness (K_{IC}) and strain energy release rate (G_{IC}) were examined based on ASTM D5045 and calculated as follows:

$$K_{IC} = (\frac{P}{BW^{1/2}})f(x) \tag{1}$$

$$x = \frac{a}{W} \tag{2}$$

$$G_{IC} = \frac{(1 - v^2)K_{IC}^2}{E} \tag{3}$$

where P is the applied load, B and W are the thickness and width of the specimen, respectively, a is the crack length of the sample, v is the Poisson's ratio ($v = 0.3$ in the present work), and E is the tensile modulus, and $f(x)$ is the constant related to the crack length:

$$f(x) = 6x\frac{[1.99 - x(1 - x)(2.15 - 3.93x + 2.7x^2]}{(1 + 2x)(1 - x)^{3/2}} \tag{4}$$

The value of × should be selected such that $0.45 < a/W < 0.55$. All the mechanical properties were evaluated at 25 °C and relative humidity of 50 ± 10%. The mechanical performance of at least ten replicate specimens was evaluated and the average results are reported.

The LOI values were determined using a JF-3 oxygen index apparatus (Nanjing Jiangning Instrument Factory, China) according to ASTM D2863 using samples with dimensions of 130 mm × 6.5 mm × 10 mm. The UL-94 vertical burning tests were conducted according to ASTM D3801 on a CZF-2 burning tester (Nanjing Jiangning Instrument Factory, China)using specimens with dimensions of 130 mm × 13 mm × 3 mm. The combustion properties of samples (100 mm × 100 mm × 3 mm) were evaluated using a cone calorimeter (Fire Testing Technology, East Grinstead, U.K) according to ISO 5660. The samples were exposed under a radiant cone at a heat flux of 35 kW/m^2. Two parallel tests were conducted on each sample. To analyze the evolved gas species, a TGA (Q5000 IR thermogravimetric analyzer) was connected to a Nicolet 6700 FTIR spectrophotometer operated under nitrogen atmosphere. The measurements were heated from 40 to 700 °C at a heating rate of 10 °C/min with a flowing rate of 50 mL/min. Py-GC/MS analysis was conducted using a Perkin-Elmer
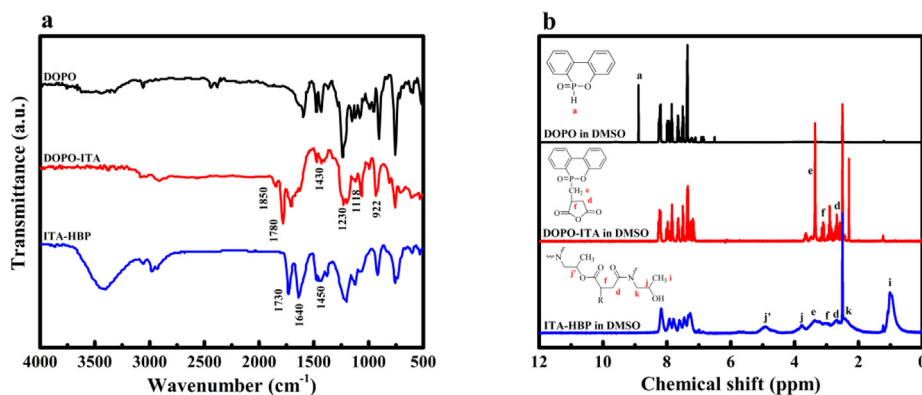
Fig. 1. FTIR (a) and ¹H NMR spectra (b) of DOPO, DOPO-ITA and ITA-HBP.
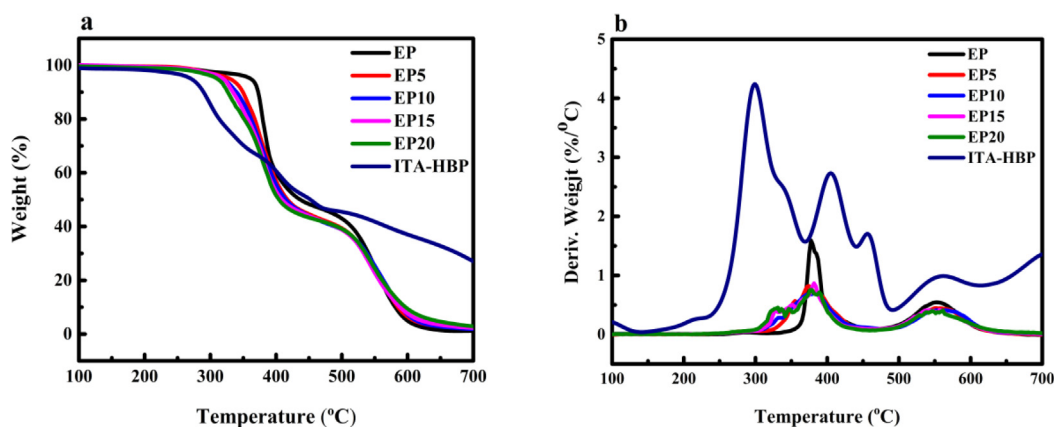

Fig. 2. TGA curves of ITA-HBP and epoxy thermosets under air atmosphere.

Table 2
Thermal decomposition parameters of ITA-HBP and epoxy thermosets under air atmosphere.

Sample	$T_{5\%}$ (°C)	$T_{50\%}$ (°C)	T_{max1} (°C)	T_{max2} (°C)	Residue at 700 °C (wt %)
ITA-HBP	270	452	299	562	27.05
EP	360	435	383	550	1.23
EP5	330	417	382	554	1.47
EP10	320	414	376	557	1.89
EP15	320	409	370	557	2.27
EP20	311	406	362	561	2.88

Clarus 680 GC-SQ8MS gas chromatography-mass spectrometer and a pyrolyzer (CDS 5200) under helium atmosphere. The injector temperature was first maintained at 40 °C for 3 min Then, the temperature

was increased to 280 °C (10 °C/min) and held there for 5 min. The interface temperature was 280 °C and the cracker temperature was 500 °C. The fractured surfaces of the samples after impact tests and morphology of residues after cone calorimeter tests were observed on a SU8010 scanning electron microscope (SEM; Hitachi, Japan). X-ray photoelectron spectroscopy (XPS) was conducted on a VG Multilab 2000 spectrometer (VG Inc.) with Al Kα excitation source.

3. Results and discussion

3.1. Structural characterizations of ITA-HBP

The FTIR spectra of DOPO, DOPO-ITA and ITA-HBP are presented in Fig. 1a. The P−O−Ph, P = O, and P-Ph stretching vibrations are detected at 922, 1230, and 1118 cm⁻¹, respectively, in the FTIR spectrum
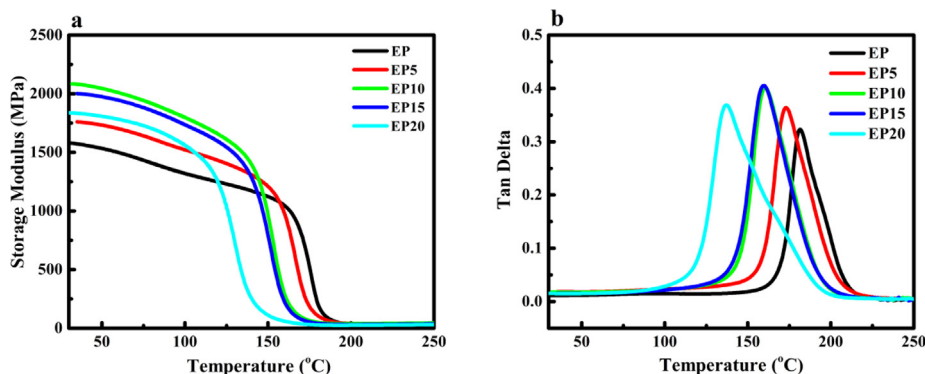

Fig. 3. Effect of ITA-HBP content on the dynamic mechanical properties of epoxy thermosets (a. storage modulus and b. tanδ).
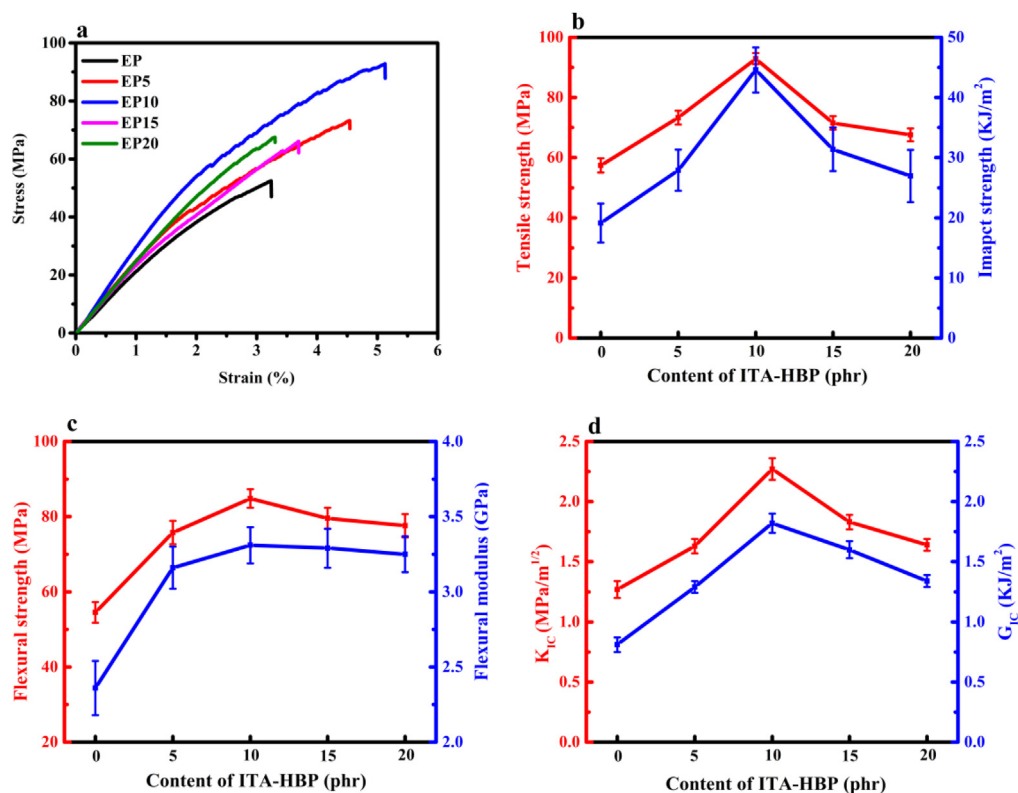
Fig. 4. Effects of ITA-HBP content on the mechanical properties of epoxy thermosets (a. tensile stress–strain curves, b. tensile strength and impact strength, c. flexural strength and flexural modulus, and d. fracture toughness and fracture energy.

Table 3
PALS data and free volume fractions of epoxy thermosets.

Sample	Lifetime of ortho-positronium τ_3 (ns)	Intensity I_3 (%)	R (Å)	Free volume fraction, Fv (%)
EP	2.064 ± 0.024	10.878 ± 0.235	1.2423 ± 0.024	1.57
EP5	2.067 ± 0.023	11.164 ± 0.231	1.2433 ± 0.023	1.62
EP10	2.084 ± 0.020	11.579 ± 0.194	1.2489 ± 0.020	1.70
EP15	2.098 ± 0.021	12.12 ± 0.212	1.2533 ± 0.021	1.80
EP20	2.130 ± 0.020	13.031 ± 0.219	1.2633 ± 0.020	1.98

of DOPO-ITA confirm the presence of the phosphaphenanthrene groups in DOPO-ITA. The peaks at 1780 and 1850 cm^{-1} are assigned to the C=O stretching and 5-member anhydride unit, respectively. The spectrum of DOPO-ITA does not have, the characteristic peaks representing the P-H stretching absorption observed for DOPO at 1430 and 1710 cm^{-1} (related to C=C double bonds. In the spectrum of ITA-HBP, the peaks at 1730 and 1640 cm^{-1} correspond to C=O stretching and cyclic anhydride groups, respectively; the C−N stretching (O=C−N−) appears at 1450 cm^{-1}, and the peak at 1640 cm^{-1} is attributed to the amide deformation.

The ^{1}H NMR spectra of DOPO, DOPO-ITA and ITA-HBP are shown in Fig. 1b. Comparison of the spectra of DOPO and ITA-HBP indicates, the peak at 8.89 ppm corresponding to −PH=O disappears in the spectrum of ITA-HBP. The peaks at 7.10–8.30 ppm confirm the presence of the phosphaphenanthrene rings. The peaks of the protons of the −CH−O− group appear at 4.40–5.20 ppm ($H_{j'}$) and those of the −CH−OH appears at 3.60–4.10 ppm (H_j). The peaks of the protons of −CO−CH− appear at 2.90–3.10 ppm (H_f), −CH$_2$−CO− appear at 2.50–2.90 ppm (H_d) and −N−CH$_2$− appear at 1.60–2.50 ppm (H_k). The peaks of the −CH$_3$ protons appear at 0.40–1.20 ppm (H_i). Fig. S1 is the ^{31}P NMR spectra of DOPO, DOPO-ITA, ITA-HBP. Further, the ^{31}P NMR spectra of DOPO, DOPO-ITA, and ITA-HBP are presented in Fig. S1. The ^{31}P NMR spectrum of DOPO-ITA clearly shows a new peak at 36.08 ppm from the P-CH$_2$ group, being related to the addition reaction between

DOPO and ITA. Meanwhile, the ^{31}P NMR spectrum of ITA-HBP shows a single peak at 35.52 ppm. The molecular weight of ITA-HBP measured by GPC (M_n) is 1698 g·mol^{-1} with a polydispersity of 2.67 (Fig. S2). All these results demonstrate the successful formation of ITA-HBP.

3.2. Thermal analysis of ITA-HBP and epoxy thermosets

Fig. 2 shows the TGA curves of ITA-HBP and ITA-HBP/epoxy thermosets and the related parameters are presented in Table 2. Obviously, ITA-HBP decomposed in the range of 220–456 °C, which matches with the decomposition temperature range of epoxy resin. The residual weight of ITA-HBP was found to be ~8.28 wt% at 700 °C, indicating that the majority of the additive decomposed into volatile products. This result indicates that ITA-HBP produced volatiles with gas-phase flame retardant activity during the combustion of the epoxy resin. The degradation of neat epoxy resin typically occurs in two stages. The first stage of decomposition occurs in the temperature range of 330–460 °C; it is related to the scission of the epoxy resin and the formation of chars at the end of the specified temperature range. In the second stage of decomposition occurring between 460 and 650 °C, thermal oxidative decomposition of the chars formed in stage 1 takes place. The ITA-HBP/ epoxy thermosets also exhibit a two stage degradation behavior, similar to that of the neat epoxy resin. However, the $T_{5\%}$ and T_{max1} of the ITA-HBP/epoxy thermosets are lower than those of neat epoxy resin,
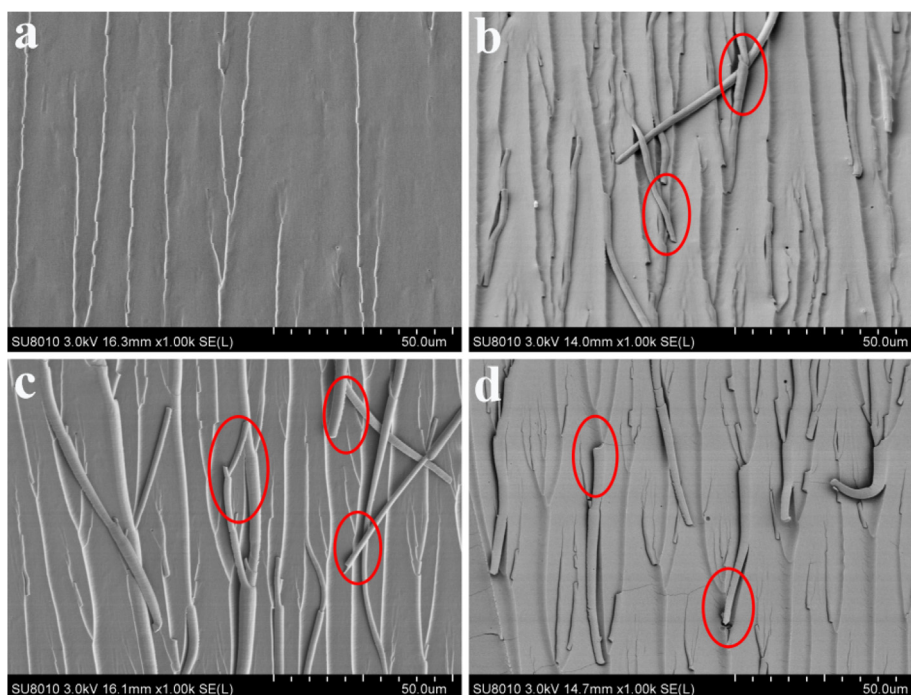
Fig. 5. SEM images of the fractured surfaces of epoxy thermosets after impact tests (a. EP, b. EP5, c. EP10, and d. EP20).

Table 4
UL-94 rating and LOI values of epoxy thermosets.

Sample	LOI (vol%)	Vertical buring test			
		After-flame time		Dripping	UL-94 rating
		t_1 (s)	t_2 (s)		
EP	26.4	52.3	–	Yes	No rating
EP5	36.4	3.3	3.0	No	V-0
EP10	37.4	2.6	1.4	No	V-0
EP15	41.6	1.8	1.1	No	V-0
EP20	42	0.8	0.8	No	V-0

indicating that ITA-HBP/epoxy thermosets could decompose at a lower temperature. In general, the earlier initial decomposition of the phosphorus-containing additives acilitates the formation of a protective char that protects the polymer matrix from flame [42]. This conclusion is supported by the increase in the char yield of the composite 700 °C (see Table 2). Compared with that of neat epoxy resin (1.23%), the char yield of the ITA-HBP/epoxy thermoset increased to 2.88% at an ITA-HBP loading of 20 phr. Furthermore, the maximum mass loss rate of ITA-HBP/epoxy thermosets was higher than that of the neat epoxy resin, and it decreased with increasing content of ITA-HBP, which is consistent with the condensed-phase flame retardant mechanism. The incorporated ITA-HBP promoted the formation of the char layer of
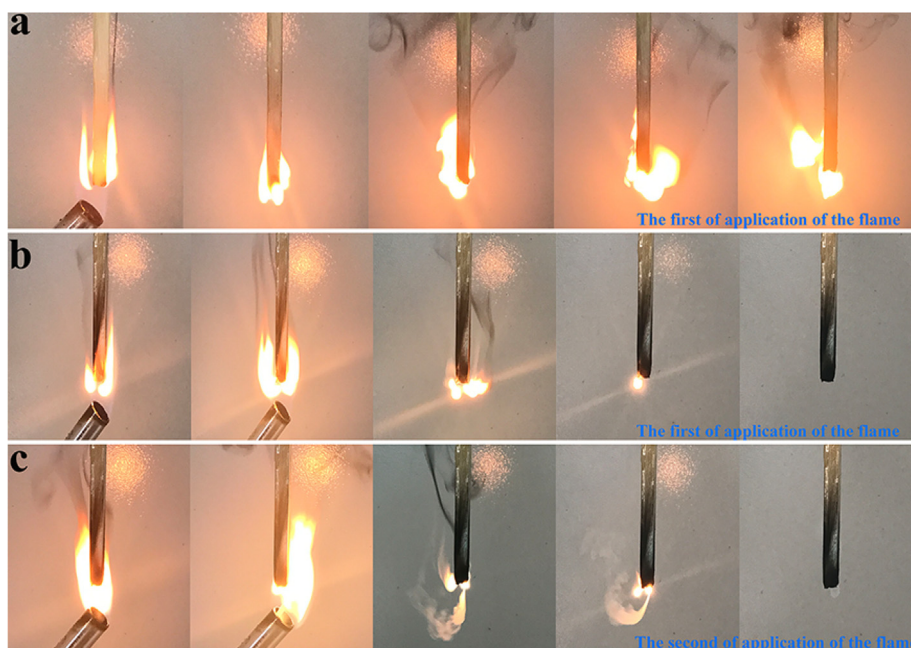

Fig. 6. Photographs of the samples captured during the UL-94 burning tests (a. EP, b. and c. EP20).
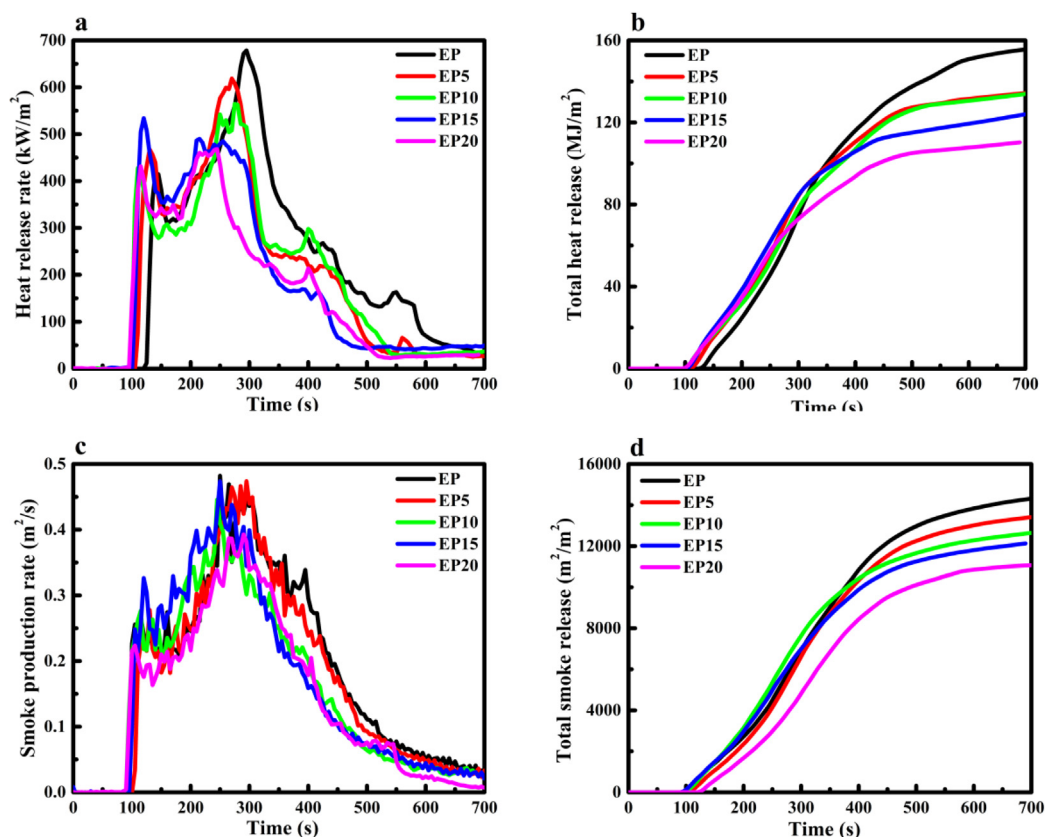
Fig. 7. Heat release rate (a), total heat release (b), residue weight (c), and total smoke release (d) curves of epoxy thermosets.

Table 5
Burning parameters of epoxy thermosets obtained from cone calorimeter tests.

Sample	TTI (s)	pk-HRR (kW/m^2)	av-EHC (MJ/m^2)	THR (MJ/m^2)	av-COY (kg/kg)	av-CO$_2$Y (kg/kg)	TSR (m^2/m^2)
EP	120	678.7	24.6	157.9	0.073	1.788	14,441
EP5	102	618.6	22.1	135.7	0.104	1.559	13,570
EP10	96	564.5	22.0	135.3	0.108	1.452	12,751
EP15	91	534.0	20.4	125.9	0.112	1.411	12,129
EP20	90	468.0	19.2	110.2	0.120	1.328	11,159

epoxy thermosets, and also inhibited the heat and oxygen permeation, which restrained the thermal degradation process and mitigated the mass loss rate. Thus, the decomposition of ITA-HBP initiated the thermal degradation of epoxy thermosets and the decomposed products of ITA-HBP catalyzed the degradation of epoxy thermosets. The release of decomposition products is essential for efficient gas-phase flame retardancy. These results explain the gas-phase fire-inhibition mechanism of the epoxy resin incorporated with ITA-HBP.

3.3. Mechanical and dynamic mechanical properties of epoxy thermosets

The plots of storage modulus and tanδ of the epoxy thermosets as a function of temperature are shown in Fig. 3, and the results of DMA are summarized in Table S1. The ITA-HBP/epoxy thermosets exhibit higher storage modulus than that of the neat epoxy resin. The storage modulus of the ITA-HBP/epoxy thermosets first increased and then decreased with increasing ITA-HBP content. This result is attributed to the combined effect of their intramolecular cavities and cross-linking density [43]. On one hand, the storage modulus increases due to the incorporation of rigid DOPO units and the increase in the crosslinking density of the cured epoxy network. On the other hand, intramolecular cavities have a negative effect on the storage modulus of epoxy thermosets. Owing to their combined effect, the storage modulus of ITA-HBP/epoxy thermosets first increases up to an ITA-HBP loading of 10 phr and then decreases with a further increase in the ITA-HBP loading. However, the T$_g$ of ITA-HBP/epoxy thermosets decreased continuously with the introduction of more aliphatic flexible chains and intramolecular cavities with increased ITA-HBP loading.

The mechanical properties of epoxy thermosets with different ITA-HBP contents are shown in Fig. 4. The ITA-HBP had a definite effect on toughness and tensile strength of the epoxy resin. The tensile strength,

Fig. 8. Digital photographs of char residues (a. EP, b. EP5, c. EP10, d. EP15, and e. EP20).
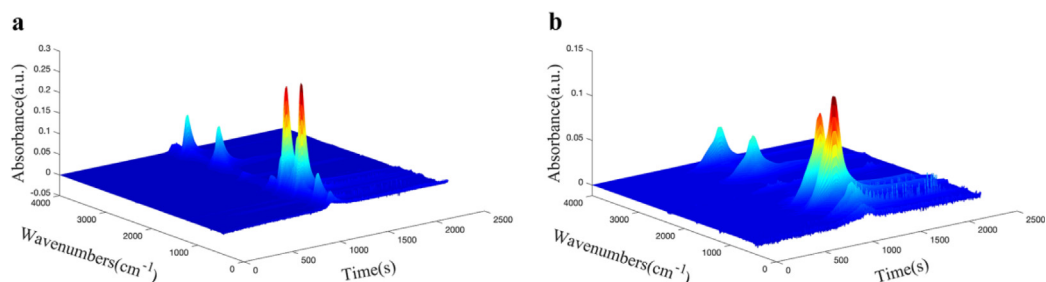
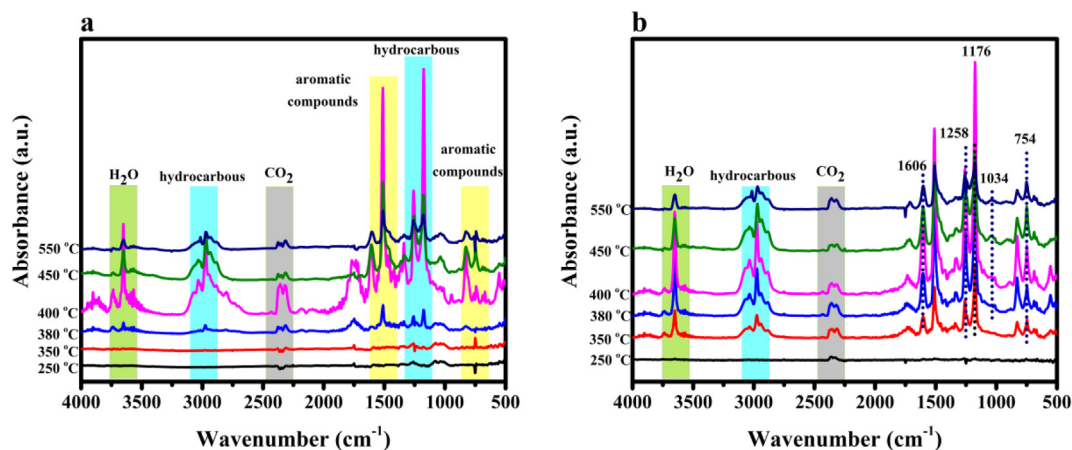**Fig. 9.** 3D TG-FTIR data of EP (a) and EP10 (b).

Fig. 10. FTIR spectra of gaseous pyrolysis products formed at different temperatures (a. EP and b. EP10).
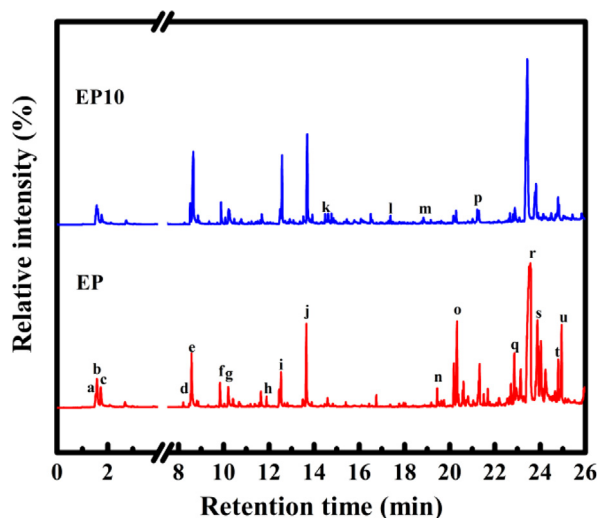

Fig. 11. Typical Py-GC/MS spectra of epoxy thermosets.

impact strength, flexural strength and toughness of epoxy thermosets followed the same pattern; they first increased and then decreased with an increase the ITA-HBP content. When ITA-HBP loading reached 10 phr, the maximum values of mechanical properties were maximized. The tensile strength, flexural strengths, impact strength, K_{IC} and G_{IC} of ITA-HBP/epoxy thermosets are respectively 37.8, 55.6, 133.2, 78.7, and 124.7% higher than those of the neat epoxy resin. The addition of ITA-HBP with intramolecular cavities increases the fractional free volume of epoxy thermosets. The increasing fractional free volumes of epoxy thermosets contributed to the enhancement of the toughness of epoxy thermosets [44,45]. The improvement in mechanical properties of epoxy thermosets may be partially also attributed to the engagement of partial -NH- groups during curing epoxy matrix. Furthermore, the

crosslinking density of epoxy thermosets increased with an increase in the added ITA-HBP, which led to higher tensile and flexural strength. As the intramolecular cavities and cross-linking density have the opposite effects, the mechanical properties of ITA-HBP/epoxy thermosets are maximized at an optimum content of ITA-HBP, 10 phr.

3.4. Toughening mechanism

In general, the incorporation of hyperbranched polymers with molecular-scale cavities into epoxy resins can lead to an e effective increase of their free volumes. PALS measurements have been performed to quantify the free volumes of hyperbranched polymer-modified epoxy thermosets [46]. The free volume fraction (F_v) can be expressed as [47–48]:

$$F_v = cVI_3 \qquad (5)$$

where I_3 is the lifetime of the intensity, V is the total volume of a single site of free volume or cavity, which can calculated from τ_3 (lifetime of ortho-positronium) and c is an empirical constant, which is usually set to $0.018 \pm 0.002\,nm^{-3}$ for polymers. The τ_3 values correspond to the size of the individual free volume sites and the relevant results are listed in Table 3. The addition of ITA-HBP leads to an increase in the size and concentration of free volume sites in epoxy thermosets. Increasing the ITA-HBP leads to an content leads to a monotonic increase in the increase the free volume fraction of epoxy thermoset, owing to the molecular-scale intramolecular cavities of ITA-HBP. The free volume size and the number of free volume units of epoxy resins incorporated with ITA-HBP are much larger than those of the neat epoxy resin. That is, the incorporated ITA-HBP increases the free volume of epoxy thermosets. The free volume fraction reaches the maximum value (1.98%) at an ITA-HBP content of 20 phr, with the corresponding free volume fraction being 26.1% higher than that of the neat epoxy resin. In general, an epoxy resin with a higher free volume fraction has more space for segmental motion, and the segmental motion of epoxy chains is thus

Table 6
Structural assignments for the main fragments observed in the Py-GC/MS of epoxy thermosets.
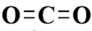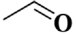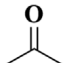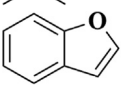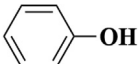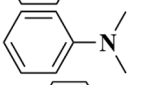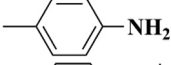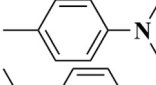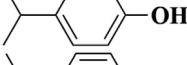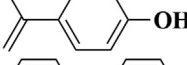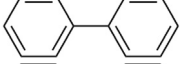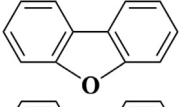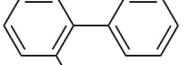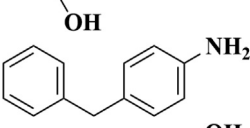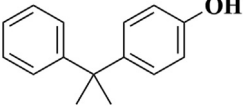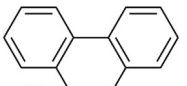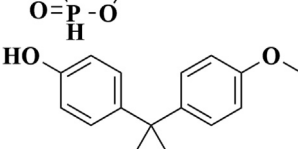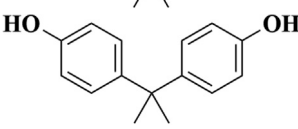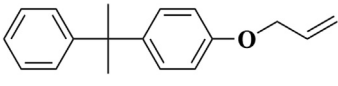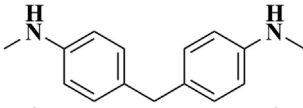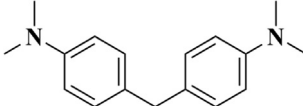
No.	m/z	Assigned structure	Relative area (%) EP	EP10
A	44	O=C=O	1.49	2.90
B	44	(aldehyde structure)	3.33	2.24
C	58	(ketone structure)	2.22	1.26
D	118	(benzofuran structure)	1.39	3.22
e	94	(phenol, –OH)	6.43	11.05
f	121	(N,N-dimethylaniline structure)	3.02	3.55
g	107	(–NH₂ substituted)	2.40	2.26
h	135	(N structure)	1.26	0.20
i	136	(–OH structure)	4.17	11.06
j	134	(–OH structure)	10.26	14.34
k	154	(biphenyl structure)	–	1.55
l	168	(dibenzofuran, O)	–	1.29
m	170	(–OH biphenyl structure)	–	0.93
n	183	(–NH₂ structure)	2.22	0.24
o	212	(–OH structure)	10.25	1.89
p	216	(O=P–O H structure)	–	1.89
q	242	(HO ... O structure)	6.10	2.14
r	228	(HO ... OH structure)	17.09	26.31
s	252	(O allyl ether structure)	8.79	5.59

Table 6 (continued)

No.	m/z	Assigned structure	Relative area (%) EP	EP10
t	240	(diamine structure)	5.20	3.70
u	254	(diamine structure)	9.64	2.40

promoted. Thus, more impact energy can be absorbed or dissipated when the material is subjected to mechanical stress [49,50]. These results imply that the toughness of epoxy resins can be significantly improved by incorporating ITA-HBP.

Fig. 5 shows the fractured surfaces of epoxy thermosets after impact tests. The neat epoxy resin shows a smooth and featureless surface (Fig. 5a), reflecting a typical brittle fracture. On the other hand, the ITA-HBP/epoxy samples show fractured morphologies, with surface characteristic ranging from smooth to rough with visible protonemata. The protonema are indicated by red circles. This is the evidence that the improvement in the toughness of epoxy thermosets is due to the *in-situ* reinforcing and toughening mechanism described in our previous work [51]. The nano-sized cavities introduced into the epoxy resin by the incorporation of ITA-HBP increase the fractional free volume of the epoxy thermosets, and in turn increase the shear yielding of the epoxy matrix surrounding ITA-HBP. The plastic deformation of the epoxy matrix led to the dissipation of the strain energy and absorption of the crack energy induced by the shear yielding. Thus, the introduction of ITA-HBP into the epoxy resin led to effective improvement of the toughness of the epoxy thermosets.

3.5. UL-94 and LOI analysis

The results of LOI and UL-94 tests are presented in Table 4. The neat epoxy resin exhibited intrinsic inflammability with a LOI of 26.4% and failed the UL-94 test. The incorporation of ITA-HBP led to a significant increase in the LOI of the epoxy resin up to 42%. The LOI increased with increasing content of ITA-HBP in the epoxy resin. Therefore, the flame retardancy of epoxy thermosets was significantly enhanced at low phosphorus contentS. The incorporation of as little as 5 phr ITA-HBP (phosphorus content of 0.26 wt%) increased the LOI of the epoxy thermoset from 26.4 to 36.4%, and the material scored V-0 rating. With a further increase in the ITA-HBP content to 15 phr lifted the LOI value to 41.6%. However, when the ITA-HBP content was increased to 20 phr, there was little further increase in the LOI.

The burning behaviors of epoxy thermosets were recorded with a digital camera to further investigate the flame retardancy of epoxy thermosets. Fig. 6 shows some video screenshots obtained during the combustion of the epoxy thermosets. The neat epoxy resin (Fig. 6a) failed to self-extinguish in 10 s after ignition and showed severe smoking and melt dripping. Thus, the neat epoxy resin did not pass the UL-94 test. On the other hand, the ITA-HBP/epoxy thermoset containing 0.26 wt% phosphorus (5 phr ITA-HBP) self-extinguished within 10 s after the fire source was taken away, and scored a UL-94 V-0 rating with no melt dripping and lesser smoking. These results suggest that ITA-HBP significantly improves the self-extinguishing performance of the epoxy resin.

3.6. Cone calorimetric analyses

Fig. 7 presents the curves of heat release rate (HRR), total heat
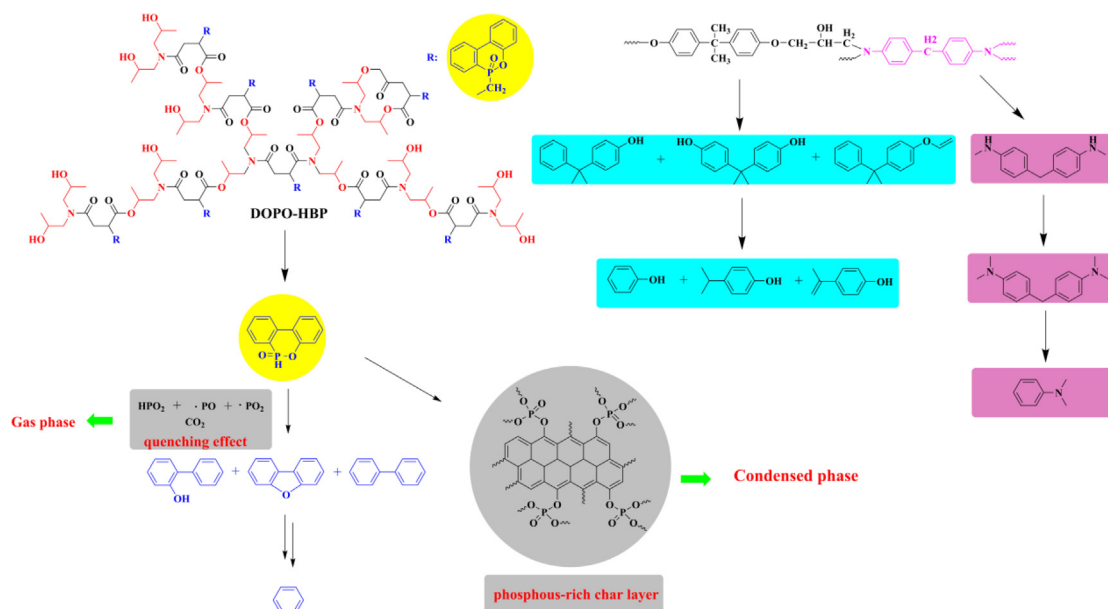
Scheme 2. Proposed pyrolysis mechanism and flame retardant mechanism of ITA-HBP/epoxy thermosets.
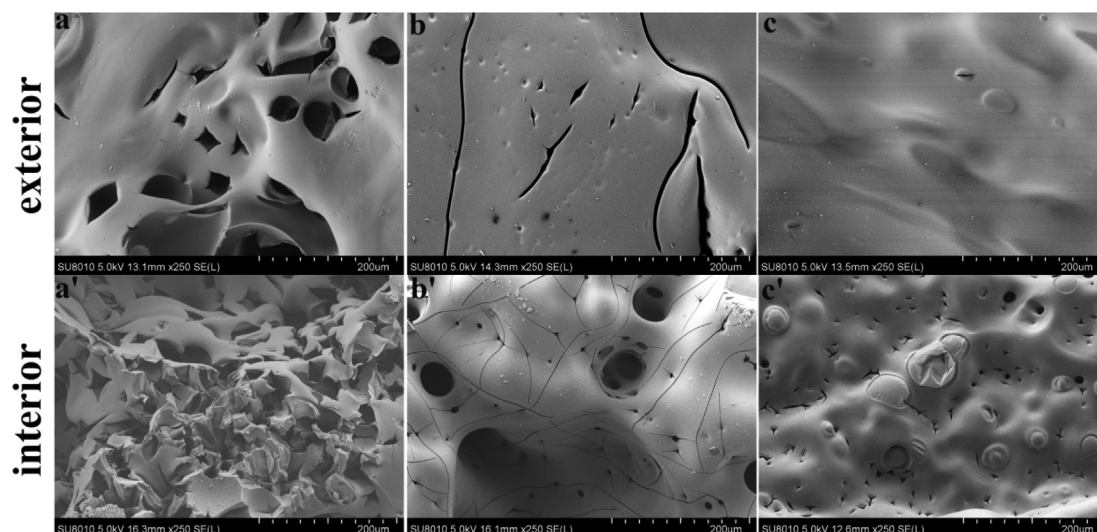

Fig. 12. SEM micrographs of the exterior and interior char residues after the cone calorimeter test of EP (a and a′), EP10(b and b′) and EP20 (c and c′).

release (THR), residue weight, and total smoke release (TSR) of the ITA-HBP thermosets, and Table 5 summarizes the characteristic parameters. The HRR curves in Fig. 7a indicate that the neat epoxy resin burned quickly immediately after being sparked and the heat release rate sharply increased to a maximum value of 678.7 kW/m², while the total heat rate (THR) increased a maximum of 157.9 MJ/m². The incorporation of ITA-HBP led to a significant reduction in the HRR, THR and TSR of ITA-HBP/epoxy thermosets, indicating the high flame-retarding effect of ITA-HBP. The TTIs of ITA-HBP/epoxy thermosets decreased with an increase in the content of ITA-HBP from 5 to 20 phr, all the TTIs were shorter than that of the neat epoxy resin. During the initial degradation, free radicals are produced by the decomposition of ITA-HBP at a lower temperature. The so-produced free radicals induce the pyrolysis of the epoxy matrix and the release of volatile species. Thus, the ignition-resistance of ITA-HBP/epoxy thermosets weakens and the TTIs decrease. The av-EHC value of ITA-HBP/epoxy thermosets is lower and the char yield after combustion is higher compared to those of the neat epoxy. The lower heat of combustion during the burning process can be attributed to the incomplete combustion of volatile products because of the gas-phase fire-inhibition activity of

ITA-HBP. The ITA-HBP as gas-phase flame retardancy of ITA-HBP may be explained by the vapor-phase flame retardant mechanism. The lower heat of combustion in the burning process is associated with gas-phase fire-inhibition activity and could be attributed to the incomplete combustion of volatile species. Thermal analysis suggested that volatile products are produced by the decomposition of ITA-HBP. The production of volatile species is very important in the oxygen-capture and oxygen-dilution processes, which improve the ignition-resistance of epoxy thermosets. This is responsible for the increase in the av-COY and decrease in the av-CO₂Y. The pk-HRR, THR and av-EHC values of ITA-HBP/epoxy thermosets loaded with 20 phr ITA-HBP decreased significantly to 468.0 kW/m², 110.2 MJ/m² and 19.2 MJ/m², respectively, and the TSR decreased from 14,441 to 11,159 m²/m². These results indicate effective reduction of the amount of noncombustible gases released from ITA-HBP. The noncombustible gases contribute to the generation of an intumescent char layer, while the released gases take away volatile fragments from the surface of the burning matrix. In addition, ITA-HBP could promote the decomposition of the epoxy matrix into phenol, toluene, and other small fragments, which exist in gaseous state rather than as particles. Thus, the fire-inhibition activity
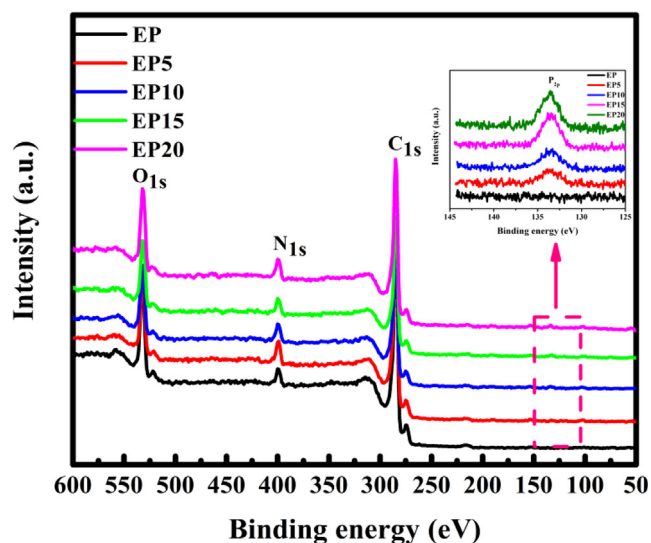
Fig. 13. Survey-scan XPS spectra of epoxy thermosets after the cone calorimeter tests.

Table 7
The elemental contents of the residues of epoxy thermosets after cone calorimeter tests.

Samples.	Element concentration (%)			
	C	O	N	P
EP	80.81	14.43	4.76	0.00
EP5	78.89	13.52	6.94	0.66
EP10	78.70	13.75	6.78	0.77
EP15	78.04	14.42	6.38	1.15
EP20	77.07	15.10	6.75	1.09

of ITA-HBP/epoxy thermosets in the gas phase was improved.

Photographs of the residual chars of epoxy thermosets after cone calorimeter tests are shown in Fig. 8. The fragmentary residue of the neat epoxy resin was thin and could not cover the underlying foil (Fig. S4a), whereas ITA-HBP/epoxy thermosets produced larger volume of residual char, which was thicker and more intumescent (Fig. 8b–d). The residual char of epoxy thermosets could essentially shield the underlying epoxy matrix from the radiated heat.

3.7. TGA-FTIR analysis

Fig. 9 presents the 3D TG-FTIR spectra of the gaseous phases evolved during the thermal decomposition of epoxy thermosets. The characteristic spectra at different temperatures are shown in Fig. 10. The major components of degradation products were methyl-substituted compounds ($2940 \, cm^{-1}$) and aromatic ones (1612 and $1510 \, cm^{-1}$). The major thermal degradation products of the neat epoxy resin are compounds containing $-OH$ ($3500–3650 \, cm^{-1}$), CO_2 ($2360 \, cm^{-1}$) and aromatic compounds ($1510 \, cm^{-1}$). The FTIR spectra of the gases evolved from the ITA-HBP/epoxy thermosets displayed characteristic bands of H_2O or phenol ($3652 \, cm^{-1}$), CO_2 ($2360 \, cm^{-1}$), $C=O$ stretching vibration of the ester group ($1730 \, cm^{-1}$), bands of compounds containing aromatic rings (3034, 1510 and $826 \, cm^{-1}$) and hydrocarbons $-CH_2$- and $-CH_3$ vibrations of hydrocarbons (1100–1300 and $2800–3100 \, cm^{-1}$). The new peak observed at $1034 \, cm^{-1}$ in the spectra of EP10 between 350 and 380 °C corresponds to -P-O-P vibration. Other vibrational peaks, such as $1606 \, cm^{-1}$ (-P-O-Ph), $1258 \, cm^{-1}$ (PO), $1176 \, cm^{-1}$ (-P-O-P-O) and $754 \, cm^{-1}$ (o-phenylphenol), are also observed. These results suggest that the degradation of ITA-HBP results in polyphosphate structures, and forms P-O-Ph bonds are formed

through their reaction with other degradation products (phenol or bisphenol).

3.8. Pyrolysis behaviors of epoxy thermosets

The Py-GC/MS spectra of epoxy thermosets are shown in Fig. 11 and the products of pyrolysis are listed in Table 6. The proposed pyrolysis routes for ITA-HBP/epoxy thermosets are shown in Scheme 2. The m/z value of fragments at 94 (phenol), 134 (4-isopropenylphenol). 136 (4-isopropyl phenol), 212 (4-(2-phenyl propan-2-yl)) and 228 (4-(2-(4-hydroxyphenyl)propan-2-yl)phenol) in the Py-GC/MS spectra are derived from the aromatic ring opening reaction and rearrangement reaction of the bisphenol A chanis. The peaks at m/z 107, 183, 240, and 254 are attributed to the volatiles, *N*-methylbenzenamine, 4-(4-(methylamino)benzyl)-*N,N*-dimethylbenzenamine, and 4-(4(dimethylamino)benzyl)-*N,N*-dimethylbenzenamine, resulting from the pyrolysis of 4,4′-diaminodiphenylmethane. As the epoxy thermosets contain phosphaphenanthrene group, the m/z values of the fragments at 154, 168 and 170 are attributed to diphenyl, dibenzofuran and o-phenylphenol, respectively [52,53]. The decomposition of ITA-HBP results in the liberation of PO_2 and PO radicals during the combustion process, and these radicals could capture H and O radicals in the gas phase and effectively delay the decomposition and burning of the epoxy matrix. Meanwhile, the produced nonflammable gases such as CO_2, N_2, NH_3 and NO_2 dilute ignitable gases, cut off the supply of oxygen, and take away the heat during the combustion of the epoxy thermosets. The residual phosphorus in the condensed phase favors carbonization, thus promoting the formation of a higher amount of residual char. Consequently, the intumescent char layer prevents the underlying material from continuously degrading, which results in increased flame retardancy and residual char of ITA-HBP/epoxy thermosets.

3.9. Morphologyand chemical structure of the residual char

Fig. 12 presents the morphology of the residual char obtained from the epoxy thermosets after the cone calorimeter test. Many micro-sized cracks and pits can be observed on the char layer of the neat epoxy resin. On the other hand, the exterior char layers of the ITA-HBP/epoxy thermosets show continuous compact structures, which reflect the strong quenching effect and dilution of the released free radicals. Some holes were formed on the surface of ITA-HBP/epoxy thermosets. Several bubbles separated by thin layers can also be observed in the interior char residues, which have intumescent characteristics and a honeycomb structure; they enhance heat exchange and oxygen-exchange. Therefore, the combination of the barrier effect and quenching effect enhanced the flame retardancy of the epoxy thermosets.

The chemical components of the external char layer of the epoxy thermosets were analyzed by XPS (Fig. 13). The atomic percentages of the various elements are given in Table 7. Owing to the highly oxidized exterior of the char in the rich oxygen environment, the carbon element content in the char of the ITA-HBP/epoxy thermosets was found to be lower than that in the char of the neat epoxy resin. Further, the oxygen content in the char residue of ITA-HBP/epoxy thermosets was found to be lower than that of the neat epoxy resin, indicating that ITA-HBP promoted the formation of char residues and increased the thermal oxidative resistance of the char layer. Numerous P species were observed in the char of ITA-HBP/epoxy thermosets, indicating its high flame-retarding performance in the condensed phase and the quenching effect of ITA-HBP. The phosphorus-based free radicals are released into the gas phase during combustion. At high temperatures, ITA-HBP promotedthe formation of char yield and enhanced the thermal oxidative stability of the formed char layer on the surface. The formed char layer could effectively slow down the heat transfer and isolate oxygen from the underlying epoxy substrate, thus restraining further combustion of the material.

The high-resolution C_{1s}, N_{1s}, and P_{2p} XPS of the external char of
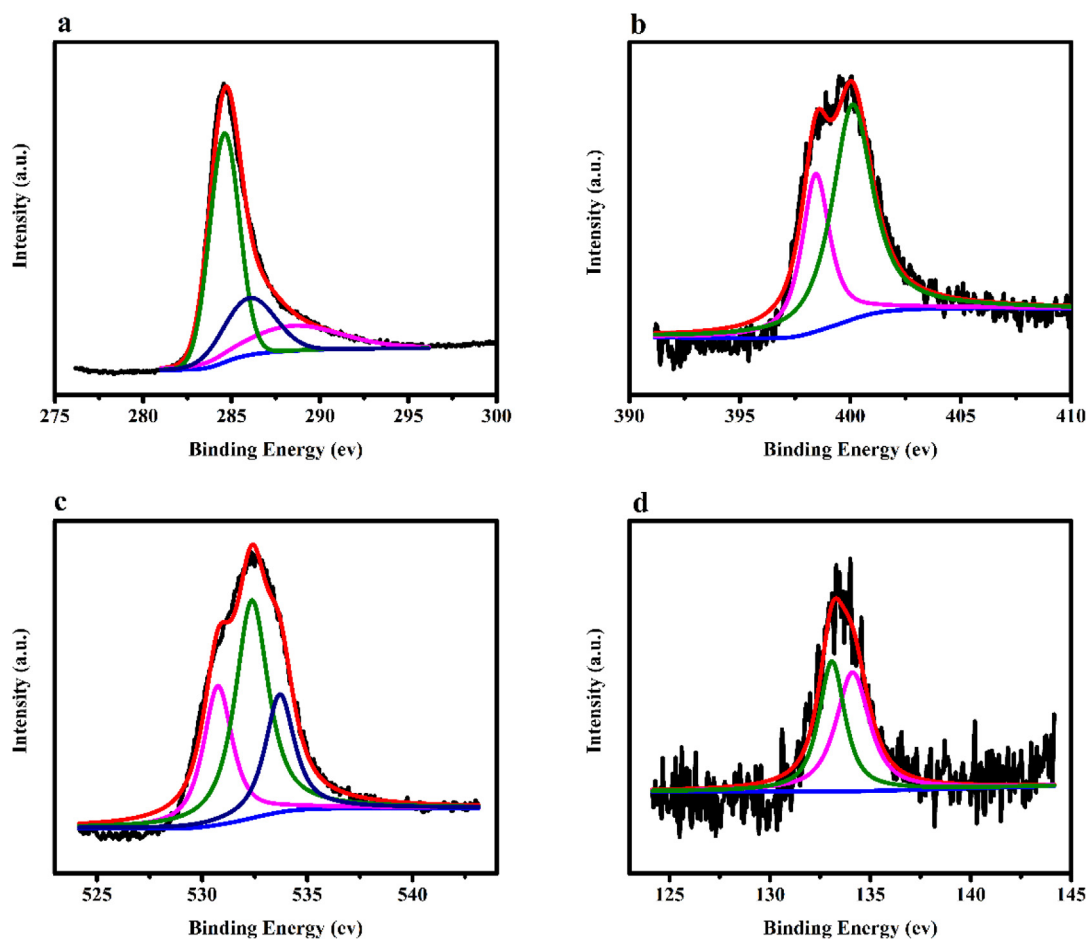
Fig. 14. XPS spectra of the external char of EP10 after the cone calorimeter test (a. C_{1s}, b. N_{1s}, c. O_{1s} and d. P_{2p}).

EP10 are displayed in Fig. 14. The C_{1s} spectrum could be deconvoluted into three main peaks at 288.7 (carbonyl groups), 286.1 (C-O in ether and/or hydroxyl group) and 284.6 eV (C–C in aliphatic and aromatic species). In the O_{1s} spectrum, the deconvoluted peaks at 533.7, 532.4 and 530.8 eV can be assigned to C−OH, −O− in C−O−C or C−O−P and =O in phosphate or carbonyl groups, respectively. The N 1 s spectral peak could be resolved into two components at 400.1 and 398.5 eV, corresponding to oxidized nitrogen compounds and imide nitrogen, respectively. In the P_{2p} spectrum, the single peak at 133.3 eV can be assigned to polyphosphate and pyrophosphate. The results indicate that ITA-HBP could produce polyphosphorus acid and phosphorus during the combustion of epoxy thermosets, which contributes to the formation of carbonaceous protective layers through dehydration and esterification of the epoxy thermosets.

3.10. Mechanism of flame retardancy

Essentially, the flame retardancy of the resulting epoxy thermosets can be attributed to the efficient flame-retarding effect of ITA-HBP in both gas and condensed phases, and the flame retardant mechanism was shown in Scheme 2. Phosphorus radicals, PO2 and PO free radicals are produced during the degradation of ITA-HBP. As the combustion continues, more phosphorus species are generated in the carbon layers, which catalyze the dehydration of epoxy thermosets. This supposition is supported by the fact that the char residues of ITA-HBP/epoxy thermosets contain higher phosphorus contents than that of the neat epoxy resin. The PO2 and PO free radicals quench the active free radicals and thus restrain the intensity of burning. The free radical chain reactions during the combustion are rapidly quenched by PO and phenol free radicals formed by the pyrolysis of P groups. The ignitable gas is diluted

with nonflammable gases decomposed from the N groups. The flame-retardant effect of ITA-HBP is induced in two phases. In the gas phase, the quenching effect of phosphorus-based free radicals formed from the decomposition of ITA-HBP plays a major role. In the condensed phase, aromatic char layers are generated by the dehydration of phosphorous fragments. An excellent flame retardancy is achieved through the combined effect of ITA-HBP in both gaseous and condensed phases.

4. Conclusion

In summary, flame-retardant epoxy thermosets were fabricated from novel bio-based hyperbranched polymers (ITA-HBP) derived from itaconic anhydride. At a loading of 10 phr ITA-HBP, the impact strength, K_{IC}, and G_{IC} of the resulting epoxy thermosets were improved by 133.2%, 78.7% and 124.7%, respectively. When the content of ITA-HBP was increased to above 15 phr, no further enhancement of the mechanical performance occurred. The simultaneous increase in the tensile strength, flexural strength, impact strength and fracture toughness can be attributed to the *in-situ* reinforcing and toughening mechanism. The ITA-HBP also induced a remarkable improvement in the flame retardancy and smoke suppression of the epoxy thermosets at low phosphorus-contents. With the incorporation of 5 phr ITA-HBP (0.26 wt % phosphorus content), the ITA-HBP/epoxy thermoset scored a V-0 rating with the LOI being 36.3%. The ITA-HBP also effectively reduced the pk-HRR, av-EHC values and CO_2Y amount and increased the COY amount of epoxy thermosets. The significant improvement in the flame retardancy is ascribed to the flame-retarding effect of ITA-HBP in both gas and condensed phases.

Acknowledgment

Appendix A. Supplementary data

Supplementary data to this article can be found online at https://doi.org/10.1016/j.cej.2019.122719.

References

[1] Q.H. Kong, T.J.H. Wu, D.Y. Zhang, Wang, Simultaneously improving flame retardancy and dynamic mechanical properties of epoxy resin nanocomposites through layered copper phenyl phosphate, Compos. Sci. Technol. 154 (2018) 136–144.

[2] M. Gholipour-Mahmoudalilou, H. Roghani-Mamaqani, R. Azimi, A. Abdollahi, Preparation of hyperbranched poly (amidoamine)-grafted graphene nanolayers as a composite and curing agent for epoxy resin, Appl. Surf. Sci. 428 (2018) 1061–1069.

[3] S. Kumar, S. Krishnan, S.K. Samal, S. Mohanty, S.K. Nayak, Toughening of petroleum based (DGEBA) epoxy resins with various renewable resources based flexible chains for high performance applications: a review, Ind. Eng. Chem. Res. 57 (2018) 2711–2726.

[4] J. Seo, N. Yui, J.H. Seo, Development of a supramolecular accelerator simultaneously to increase the cross-linking density and ductility of an epoxy resin, Chem. Eng. J. 356 (2019) 303–311.

[5] D. Incerti, T. Wang, D. Carolan, A. Fergusson, Curing rate effects on the toughness of epoxy polymers, Polymer 159 (2018) 116–123.

[6] Y.J. Kou, W.Y. Zhou, B. Li, L. Dong, Y.E. Duan, Q.W. Hou, X.R. Liu, H.W. Cai, Q.G. Chen, Z.M. Dang, Enhanced mechanical and dielectric properties of an epoxy resin modified with hydroxyl- terminated polybutadiene, Compos. Part A Appl. Sci. 114 (2018) 97–106.

[7] M. Laurien, B. Demir, H. Buttemeyer, A.S. Herrmann, T.R. Walsh, L.C. Ciacchi, Atomistic modeling of the formation of a thermoset/thermoplastic interphase during co-curing, Macromolecules 51 (2018) 3983–3993.

[8] M. Zhao, L.H. Meng, L.C. Ma, L.N. Ma, X.B. Yang, Y.D. Huang, J.E. Ryu, A. Shankar, T.X. Li, C. Yan, Z.H. Guo, Layer-by-layer grafting CNTs onto carbon fibers surface for enhancing the interfacial properties of epoxy resin composites, Compos. Sci. Technol. 154 (2018) 28–36.

[9] S.Y. Chen, J.H. Zhang, J.L. Zhou, D.H. Zhang, A.Q. Zhang, Dramatic toughness enhancement of benzoxazine/epoxy thermosets with a novel hyperbranched polymeric ionic liquid, Chem. Eng. J. 334 (2018) 1371–1382.

[10] J.R. Han, T. Liu, C. Hao, S. Zhang, B.H. Guo, J.W. Zhang, A catalyst-free epoxy vitrimer system based on multifunctional hyperbranched polymer, Macromolecules 51 (2018) 6789–6799.

[11] J.M. Misasi, Q.F. Jin, K.M. Knauer, S.E. Morgan, J.S. Wiggins, Hybrid POSS-hyperbranched polymer additives for simultaneous reinforcement and toughness improvements in epoxy networks, Polymer 117 (2017) 54–63.

[12] D. Santiago, A. Fabregat-Sanjuan, F. Ferrando, S. De la Flor, Hyperbranched-modified epoxy thermosets: enhancement of thermomechanical and shape-memory performances, J. Appl. Polym. Sci. 134 (12) (2017) 44623.

[13] Y.M. Wang, S.F. Chen, X.C. Chen, Y.F. Lu, M.H. Miao, D.H. Zhang, Controllability of epoxy equivalent weight and performance of hyperbranched epoxy resins, Compos. Part B-Eng. 160 (2019) 615–625.

[14] J.H. Zhang, Q.H. Kong, D.Y. Wang, Simultaneously improving the fire safety and mechanical properties of epoxy resin with Fe-CNTs via large-scale preparation, J. Mater. Chem. A 6 (2018) 6376–6386.

[15] Y.J. Xu, J. Wang, Y. Tan, M. Qi, L. Chen, Y.Z. Wang, A novel and feasible approach for one-pack flame-retardant epoxy resin with long pot life and fast curing, Chem. Eng. J. 337 (2018) 30–39.

[16] J.L. Wang, C. Ma, X.W. Mu, W. Cai, L.X. Liu, X. Zhou, W.Z. Hu, Y. Hu, Construction of multifunctional MoSe2 hybrid towards the simultaneous improvements in fire safety and mechanical property of polymer, J. Hazard. Mater. 352 (2018) 36–46.

[17] W.W. Guo, X. Wang, C.S.R. Gangireddy, J.L. Wang, Y. Pan, W.Y. Xing, L. Song, Y. Hu, Cardanol derived benzoxazine in combination with boron-doped graphene toward simultaneously improved toughening and flame retardant epoxy composites, Compos. Part A Appl. Sci. 116 (2019) 13–23.

[18] Y.J. Xu, L. Chen, W.H. Rao, M. Qi, D.M. Guo, W. Liao, Y.Z. Wang, Latent curing epoxy system with excellent thermal stability, flame retardance and dielectric property, Chem. Eng. J. 347 (2018) 223–232.

[19] M.M. Velencoso, A. Battig, J.C. Markwart, B. Schartel, F.R. Wurm, Molecular fire-fighting-how modern phosphorus chemistry can help solve the challenge of flame retardancy, Angew. Chem. Int. Ed. 57 (2018) 10450–10467.

[20] H.Y. Wu, Y.T. Li, B.R. Zeng, G.R. Chen, Y.Z. Wu, T. Chen, L.Z. Dai, A high

[21] Y.B. Hou, Y.X. Hu, S.L. Qiu, L.X. Liu, W.Y. Xing, W.Z. Hu, Bi2Se3 decorated recyclable liquid- exfoliated MoS2 nanosheets: towards suppress smoke emission and improve mechanical properties of epoxy resin, J. Hazard. Mater. 364 (2019) 720–732.

[22] X. Wang, Y. Hu, L. Song, W.Y. Xing, H.D.A. Lu, P. Lv, G.X. Jie, Flame retardancy and thermal degradation mechanism of epoxy resin composites based on a DOPO substituted organophosphorus oligomer, Polymer 51 (2010) 2435–2445.

[23] Y.Z. Feng, X.W. Li, X.Y. Zhao, Y.S. Ye, X.P. Zhou, H. Liu, C.T. Liu, X.L. Xie, Synergetic improvement in thermal conductivity and flame retardancy of epoxy/silver nanowires composites by incorporating "branch-like" flame-retardant functionalized graphene, ACS Appl. Mater. Inter. 10 (2018) 21628–21641.

[24] Y. Qiu, L.J. Qian, H.S. Feng, S.L. Jin, J.W. Hao, Toughening effect and flame-retardant behaviors of phosphaphenanthrene/phenylsiloxane bigroup macromolecules in epoxy thermoset, Macromolecules 51 (2018) 9992–10002.

[25] Y.Q. Shi, T. Fu, Y.J. Xu, D.F. Li, X.L. Wang, Y.Z. Wang, Novel phosphorus-containing halogen- free ionic liquid toward fire safety epoxy resin with well-balanced comprehensive performance, Chem. Eng. J. 354 (2018) 208–219.

[26] Y. Zhang, B. Yu, B.B. Wang, K.M. Liew, L. Song, C.M. Wang, Y. Hu, Highly effective P-P synergy of a novel DOPO-based flame retardant for epoxy resin, Ind. Eng. Chem. Res. 56 (2017) 1245–1255.

[27] R.K. Jian, P. Wang, W.S. Duan, J.S. Wang, X.L. Zheng, J.B. Weng, Synthesis of a novel P/N/S- containing flame retardant and its application in epoxy resin: thermal property, flame retardance, and pyrolysis behavior, Ind. Eng. Chem. Res. 55 (2016) 11520–11527.

[28] J.L. Wang, C. Ma, P.L. Wang, S.L. Qiu, W. Cai, Y. Hu, Ultra-low phosphorus loading to achieve the superior flame retardancy of epoxy resin, Polym. Degrad. Stabil. 149 (2018) 119–128.

[29] X.S. Li, Z.L. Zhao, Y.H. Wang, H. Yan, X.Y. Zhang, B.S. Xu, Highly efficient flame retardant, flexible, and strong adhesive intumescent coating on polypropylene using hyperbranched polyamide, Chem. Eng. J. 324 (2017) 237–250.

[30] C. Ma, S.L. Qiu, B. Yu, J.L. Wang, C.M. Wang, W.R. Zeng, Y. Hu, Economical and environment- friendly synthesis of a novel hyperbranched poly(aminomethylphosphine oxide-amine) as co-curing agent for simultaneous improvement of fire safety, glass transition temperature and toughness of epoxy resins, Chem. Eng. J. 322 (2017) 618–631.

[31] S.Q. Ma, X.Q. Liu, Y.H. Jiang, L.B. Fan, J.X. Feng, J. Zhu, Synthesis and properties of phosphorus-containing bio-based epoxy resin from itaconic acid, Sci. China Chem. 57 (2014) 379–388.

[32] R. Menard, C. Negrell, M. Fache, L. Ferry, R. Sonnier, G. David, From a bio-based phosphorus- containing epoxy monomer to fully bio-based flame-retardant thermosets, RSC Adv. 5 (2015) 70856–70867.

[33] C. Li, J.T. Wan, E.N. Kalali, H. Fan, D.Y. Wang, Synthesis and characterization of functional eugenol derivative based layered double hydroxide and its use as a nanoflame-retardant in epoxy resin, J. Mater. Chem. A 3 (2015) 3471–3479.

[34] X.J. Yang, C.P. Wang, J.L. Xia, W. Mao, S.H. Li, Study on synthesis of novel phosphorus- containing flame retardant epoxy curing agents from renewable resources and the comprehensive properties of their combined cured products, Prog. Org. Coat. 110 (2017) 195–203.

[35] X.M. Zhao, D. Xiao, J.P. Alonso, D.Y. Wang, Inclusion complex between beta-cyclodextrin and phenylphosphonicdiamide as novel bio-based flame retardant to epoxy: inclusion behavior, characterization and flammability, Mater. Des. 114 (2017) 623–632.

[36] S. Wang, S.Q. Ma, C.X. Xu, Y. Liu, J.Y. Dai, Z.B. Wang, X.Q. Liu, J. Chen, X.B. Shen, J.J. Wei, J. Zhu, Vanillin-derived high-performance flame retardant epoxy resins: facile synthesis and properties, Macromolecules 50 (2017) 1892–1901.

[37] Y.J. Bai, M. De Bruyn, J.H. Clark, J.R. Dodson, T.J. Farmer, M. Honore, I.D.V. Ingram, M. Naguib, A.C. Whitwood, M. North, Ring opening metathesis polymerisation of a new bio-derived monomer from itaconic anhydride and furfuryl alcohol, Green Chem. 18 (2016) 3945–3948.

[38] Y.J. Bai, J.H. Clark, T.J. Farmer, I.D.V. Ingram, M. North, Wholly biomass derivable sustainable polymers by ring-opening metathesis polymerization of monomers obtained from furfuryl alcohol and itaconic anhydride, Polym. Chem. 8 (2017) 3074–3081.

[39] T. Okuda, K. Ishimoto, H. Ohara, S. Kobayashi, Renewable biobased polymeric materials: facile synthesis of itaconic anhydride-based copolymers with poly(L-lactic acid) grafts, Macromolecules 45 (2012) 4166–4174.

[40] J.A. Wallach, S.J. Huang, Copolymers of itaconic anhydride and methacrylate-terminated poly (lactic acid) macromonomers, Biomacromolecules 1 (2000) 174–179.

[41] S. Yamaguchi, M. Tanha, A. Hult, T. Okuda, H. Ohara, S. Kobayashi, Green polymer chemistry: lipase-catalyzed synthesis of bio-based reactive polyesters employing itaconic anhydride as a renewable monomer, Polym. J. 46 (2014) 2–13.

[42] H.X. Ma, J.J. Li, J.J. Qiu, Y. Liu, C.M. Liu, Renewable cardanol-based star-shaped prepolymer containing a phosphazene core as a potential biobased green fire-retardant coating, ACS Sustain. Chem. Eng. 5 (2017) 350–359.

[43] J.H. Zhang, S.Y. Chen, B. Qin, D.H. Zhang, P. Guo, Q.J. He, Preparation of hyperbranched polymeric ionic liquids for epoxy resin with simultaneous improvement of strength and toughness, Polymer 164 (2019) 154–162.

[44] J.H. Zhang, S.Y. Chen, Q.J. He, P. Guo, Z.J. Xu, D.H. Zhang, Toughening benzoxazines with hyperbranched polymeric ionic liquids: effect of cations and anions, React. Funct. Polym. 133 (2018) 37–44.

[45] T. Liu, Y.X. Nie, R.S. Chen, L.D. Zhang, Y. Meng, X.Y. Li, Hyperbranched polyether as an all- purpose epoxy modifier: controlled synthesis and toughening mechanisms, J. Mater. Chem. A 3 (2015) 1188–1198.

[46] W. Gong, Y.Y. Mai, Y.F. Zhou, N. Qi, B. Wang, D.Y. Yan, Effect of the degree of branching on atomic-scale free volume in hyperbranched poly[3-ethyl-3-(hydroxymethyl)oxetane]apositron study, Macromolecules 38 (2005) 9644–9649.

[47] D. Ratna, G.P. Simon, Epoxy and hyperbranched polymer blends: morphology and free volume, J. Appl. Polym. Sci. 117 (2010) 557–564.

[48] L.J. Luo, T. Qiu, Y. Meng, L.H. Guo, J. Yang, Z.X. Li, X.Z. Cao, X.Y. Li, A novel fluoro- terminated hyperbranched poly(phenylene oxide) (FHPPO): synthesis, characterization, and application in low-k epoxy materials, RSC Adv. 3 (2013) 14509–14520.

[49] Y.C. Jean, Q. Deng, T.T. Nguyen, Free-volume hole properties in thermosetting plastics probed by positron annihilation spectroscopy: chain extension chemistry, Macromolecules 28 (1995) 8840–8844.

[50] M.F. Zeng, C.Y. Lu, B.Y. Wang, C.Z. Qi, Free volume hole size of cyanate ester resin/epoxy resin interpenetrating networks and its correlations with physical properties, Radia. Phys. Chem. 79 (2010) 966–975.

[51] S.F. Chen, Z.J. Xu, D.H. Zhang, Synthesis and application of epoxy-ended hyperbranched polymers, Chem. Eng. J. 343 (2018) 283–302.

[52] L.J. Qian, L.J. Ye, Y. Qiu, S.R. Qu, Thermal degradation behavior of the compound containing phosphaphenanthrene and phosphazene groups and its flame retardant mechanism on epoxy resin, Polymer 52 (2011) 5486–5493.

[53] S. Yang, J. Wang, S.Q. Huo, L.F. Cheng, M. Wang, Preparation and flame retardancy of an intumescent flame-retardant epoxy resin system constructed by multiple flame-retardant compositions containing phosphorus and nitrogen heterocycle, Polym. Degrad. Stabil. 119 (2015) 251–259.